

Structure of the Hamiltonian of mean force

Phillip C. Burke,^{1,2,3} Goran Nakerst,⁴ and Masudul Haque⁴

¹*School of Physics, University College Dublin, Belfield, Dublin 4, Ireland*

²*Centre for Quantum Engineering, Science, and Technology, University College Dublin, Dublin 4, Ireland*

³*Department of Theoretical Physics, Maynooth University, Maynooth, Kildare, W23 F2H6, Ireland*

⁴*Institut für Theoretische Physik, Technische Universität Dresden, 01062 Dresden, Germany*

(Dated: July 10, 2024)

The Hamiltonian of mean force is an effective Hamiltonian that allows a quantum system, non-weakly coupled to an environment, to be written in an effective Gibbs state. We present results on the structure of the Hamiltonian of mean force in extended quantum systems with local interactions. We show that its spatial structure exhibits a “skin effect” — its difference from the system Hamiltonian dies off exponentially with distance from the system-environment boundary. For spin systems, we identify the terms that can appear in the Hamiltonian of mean force at different orders in the inverse temperature.

I. INTRODUCTION

The assumption of weak system-bath coupling is widespread in thermodynamics but is clearly not universally valid. There is thus considerable interest in formulating thermodynamics to include effects of non-weak coupling [1]. A central concept in this effort is that of the Hamiltonian of mean force (HMF) [2, 3], the quantum counterpart to the classical potential of mean force [4–6]. Consider a combined system in thermal equilibrium, composed of a system A and a bath/environment B , interacting via the Hamiltonian H_{AB} so that the combined Hamiltonian is $H = H_A + H_B + H_{AB}$. The system state ρ_A , obtained by tracing out B degrees of freedom, is then not a thermal Gibbs state in general and differs from $e^{-\beta H_A}$ [7–9], here β is the inverse temperature. Nevertheless, we can formally define an effective Hamiltonian H_A^* so that $\rho_A \propto e^{-\beta H_A^*}$ [10–18]. This H_A^* is the HMF. For non-negligible coupling H_{AB} , the HMF will generally deviate from the actual system Hamiltonian H_A . For extended systems with local degrees of freedom, we address the question of how H_A^* differs from H_A , in particular, the spatial dependence of this difference.

The HMF often appears implicitly in the study of thermalization in isolated quantum systems [19–25]. Any spatial segment of an isolated system (A) can be regarded

as being thermalized by the rest of the system (B), so that the expectation values of local observables having support in A are given by their expectation values in the reduced thermal state. Since the partition between A and B is arbitrary in this setup, the coupling H_{AB} is not small, and thus the thermal state to be used is $\rho_A \propto \text{tr}_B e^{-\beta H} \propto e^{-\beta H_A^*}$ rather than just $e^{-\beta H_A}$. In this context, the temperature $1/\beta$ is determined using the canonical-ensemble correspondence between energy and temperature [19, 20, 22, 24, 26–41]. The relevance of the HMF concept in this setup raises the question of the structure of the HMF in systems with local interactions. Two questions immediately arise: (1) What is the spatial structure of the HMF, i.e., of the deviation of H_A^* from H_A ? (2) What type of interactions are contained in the HMF?

We find that when β is not very large, the difference of coefficients of HMF terms from the corresponding H_A coefficients decay exponentially with distance d to the boundary between A and B , as illustrated in Fig. 1(b). This result implies a “skin effect”, illustrated in Fig. 1(a): The HMF effectively only deviates from H_A near the boundary, i.e., the ‘bath’ B has a very shallow influence in A . This is a general result, provided the total system Hamiltonian is made of local terms. For $\beta \rightarrow \infty$ (very low temperature), we show how the HMF is related to the “entanglement Hamiltonian” [42–45] which is calculated from the ground state alone. We formulate our results in terms of spin chains, which are paradigm models for extended quantum systems with local interactions. Using a perturbative framework coupled with numerical analysis, we elucidate the types of terms that can appear in the HMF and present systematics on which types of terms can appear at which order in β .

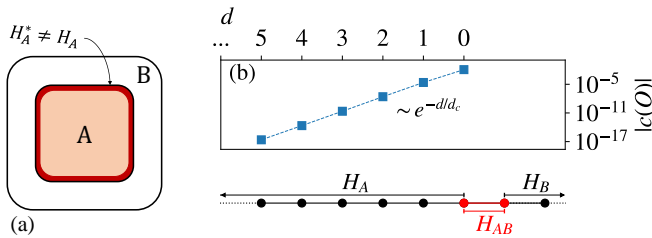


FIG. 1. (a) Illustration of the skin effect in a composite system. The dark red region indicates the shallow effect of B within A . (b) Magnitude of coefficients in the HMF plotted versus the distance d from the boundary site L_A at small β , illustrating the exponential decay with distance d .

II. DEFINITIONS & SETUP

The combined system is taken to be in a thermal state, $\rho = e^{-\beta H}/Z$, so that subsystem A (the ‘system’) is in state $\rho_A = \frac{1}{Z} \text{tr}_B e^{-\beta H}$, where tr_B is the partial trace

over B . The HMF H_A^* is defined to satisfy [2],

$$\rho_A = \frac{1}{Z^*(\beta)} e^{-\beta H_A^*(\beta)}. \quad (1)$$

This essentially defines the HMF only up to a constant [46–48]. As this freedom is not of interest to us (it only adds an identity operator to the HMF), we remove the ambiguity by choosing the normalization to be $Z^*(\beta) = Z(\beta)/Z_B(\beta)$, where Z and Z_B are the partition functions of the combined system and the subsystem B (‘bath’), respectively. With this definition, the HMF is

$$H_A^*(\beta) = -\frac{1}{\beta} \ln \frac{\text{tr}_B(e^{-\beta H})}{\text{tr}_B(e^{-\beta H_B})}. \quad (2)$$

The HMF H_A^* reduces to the bare system Hamiltonian H_A for vanishing coupling ($H_{AB} = 0$) [49–51] and for infinite temperature ($\beta = 0$) [13].

For definiteness, we formulate our results for the XXZ chain, with and without magnetic fields. This exemplifies the case of operators being supported on nearest neighbor sites (spin-spin interactions) or single sites (magnetic fields). Generalization to longer-range interactions and to fermionic or bosonic systems should be straightforward, but we do not attempt to write out explicitly all such cases. The Hamiltonian is

$$H = J \sum_{j=1}^{L-1} (\sigma_j^x \sigma_{j+1}^x + \sigma_j^y \sigma_{j+1}^y) + \Delta \sum_{j=1}^{L-1} \sigma_j^z \sigma_{j+1}^z + \sum_{j=1}^L (h_j^z \sigma_j^z + h_j^x \sigma_j^x), \quad (3)$$

where J is the site-to-site ‘hopping’ strength, Δ is the spin-spin interaction strength (anisotropy), and h_j^z , (h_j^x) denotes the strength of the on-site magnetic field in the z direction (x direction) on-site j . Unless otherwise stated, we will generally use uniform magnetic fields, i.e., $h_j^z = h^z$ and $h_j^x = h^x$, $\forall j$. The case of $h_j^z = h_j^x = 0$ is the standard XXZ chain. We take the first L_A sites as subsystem A ; the boundary bond connects sites $j = L_A$ and $j = L_A + 1$.

A convenient basis to investigate the HMF of spin systems is the basis of Pauli operators. The Pauli operators $O = \sigma_{i_1}^{\alpha_1} \dots \sigma_{i_{L_A}}^{\alpha_{L_A}}$, where $\alpha_j = \{x, y, z\}$ and i_j denote sites in A , together with the identity operator form an orthogonal basis of operators with respect to the Hilbert-Schmidt scalar product. The coefficient of an operator in a Hamiltonian is given by the scalar product of the operator with the Hamiltonian. Thus, we quantify the deviation of the HMF from H_A by

$$c(O) = \text{tr} [O \cdot (H_A^*(\beta) - H_A)], \quad (4)$$

i.e., by the difference of coefficients of the same operator in the HMF and H_A .

All numerical results in this work are obtained via exact diagonalization, i.e., the canonical density matrix of

the entire $A + B$ system is constructed explicitly as a $2^L \times 2^L$ matrix, and then the B degrees of freedom are traced out numerically. The computations are performed with 128-bit precision. This higher precision is necessary because in many cases the coefficients are orders of magnitude smaller than the precision of double-precision floating-point arithmetic ($\sim 10^{-16}$).

We refer to the B partition (sites $L_A + 1$ to L) as the ‘bath’. However, in the present setting, we are not interested in the thermalizing effect of the bath, since the full $A + B$ system is already imposed to be in a Gibbs (thermal) state. This means that the B partition is not required to have any of the properties (zero memory, fast timescales, infinite bandwidth, etc) that a physical bath is usually assumed to have. In particular, the B partition is not required to be larger than the A partition. In fact, we find that the size of the ‘bath’ does not affect the qualitative insights presented in this work. Therefore, it is computationally advantageous to take the B partition to be as small as meaningful, and we present much of our data for systems with $L = L_A + 1$, i.e., a single site in B . This might appear to contradict the usual idea of a physical bath that thermalizes a system and sets the temperature, for which a large size is necessary or at least helpful. However, in the present setting, a single-site ‘bath’ is perfectly reasonable.

III. WHICH TERMS APPEAR?

Terms appearing in H_A^* , beyond those already in H_A , are formed by combining terms in H , as can be seen by considering an expansion of Eq. (2) in β . Thus any term in H_A^* must have the form $O \equiv h_1 \dots h_k$ (equality up to a constant), with the h_i being terms that appear in H .

The type of Pauli operators appearing in H constrains the types that can appear in H_A^* . We outline the cases of an XXZ chain – other cases can be worked out analogously. For the XXZ Hamiltonian *without* magnetic fields, the operators appearing in the HMF can be identified by considering a homomorphism of the Klein four-group, the group of Pauli matrices modulo phases [52]. The homomorphisms are given by assigning a sign ± 1 to single-body Pauli operators σ^x , σ^y , and σ^z . All terms in the XXZ Hamiltonian without magnetic fields have sign $+1$, regardless of the sign function. This carries over to the corresponding HMF [52]. For single-body and mixed two-body ($\sigma_i^\alpha \sigma_j^{\alpha'}$ for $\alpha \neq \alpha'$) Pauli operators, there are sign functions such that the sign of the operators is negative. Thus, these Pauli operators do not appear in the HMF. This purely algebraic argument [52] is independent of the temperature and the lattice geometry.

The XXZ Hamiltonian with magnetic fields contains single-body Pauli operators and the above argument breaks down. The corresponding HMF overlaps with all Pauli operators for any $\beta > 0$. In table I, we list the one and two-body terms that can arise in the HMF for several system Hamiltonians.

H	σ_j^α	$\sigma_j^\alpha \sigma_{j+1}^\alpha$	$\sigma_j^\alpha \sigma_k^\alpha$	$\sigma_j^\alpha \sigma_k^{\alpha'}$
$XX (\Delta = 0)$.	✓	.	.
$XXZ (\Delta \neq 0)$.	✓	✓	.
$XXZ + \sigma_n^\alpha$	✓	✓	✓	✓
Min. order in β	β^{2d+1}	β^{2d}	β^{2d}	β^{2d+1}

TABLE I. One- and two-body terms appearing in H_A^* , for various system Hamiltonians H . The final row indicates the minimum order in β at which the terms can appear.

IV. SMALL β

For $\beta \rightarrow 0$, the HMF converges to H_A [11, 13]. For small $\beta > 0$, we find that H_A^* differs from H_A most notably close to the boundary of A with the bath B , i.e., $|c(O)|$ is larger for operators O supported close to the boundary. We define the distance $d(O)$ as the distance from the boundary to the farthest site within the support of O , i.e., for an n -body Pauli operator $O = \sigma_{i_1}^{\alpha_1} \dots \sigma_{i_n}^{\alpha_n}$ with $i_1 < \dots < i_n$, we have $d(O) = L_A - i_1$.

Remarkably, $|c(O)|$ decays exponentially with distance d from the boundary. For one-body ($n = 1$) terms, the clear exponential behavior is seen in Fig. 1(b) and Fig. 2 (a); similar exponential behaviors are observed for $n = 2$ and $n = 3$ operators [52]. This exponential decay with distance means that the HMF differs from the bare subsystem Hamiltonian H_A only by a skin effect. The skin depth d_c is defined by

$$|c(O)| \sim e^{-d/d_c}. \quad (5)$$

The skin depth is the slope in Fig. 1(b) and Fig. 2(a). The skin depth as a function of β is shown for one-, two-, and three-body terms in Fig. 2(b). This dependence is very well approximated by

$$d_c \approx \frac{1}{a - 2 \ln \beta}. \quad (6)$$

The quantity $a(O)$ is numerically found to be either independent of or at most weakly dependent on β and to depend on the operator O . The term $2 \ln \beta$ is independent of the operator; we will provide a perturbative argument below.

A. Perturbative considerations

Eqs. (5) and (6) can be justified by a perturbative argument in β . We expand the HMF in a formal power series in β ,

$$H_A^* = \sum_{k=0}^{\infty} \beta^k H_{A,k}^*, \quad (7)$$

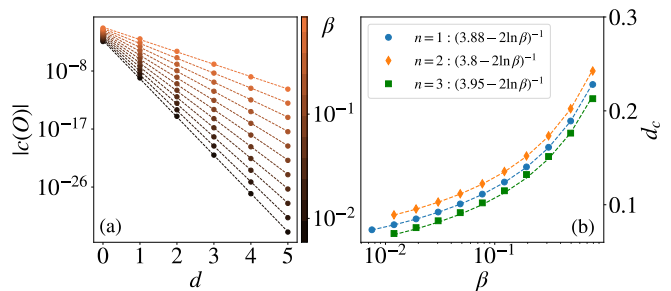


FIG. 2. (a) $|c(O)|$ for 1-body term (σ_j^α) in the HMF versus distance for various β (colorbar). Corresponding curves for 2- or 3-body terms are similar [52]. (b) Skin depth d_c as function of β , for 1-body, 2-body ($\sigma_\ell^\alpha \sigma_m^\alpha$), 3-body ($\sigma_\ell^\alpha \sigma_m^\alpha \sigma_n^\alpha$) terms. $n = 1$ corresponds to slopes in (a). Dashed lines are $(a - 2 \ln \beta)^{-1}$ for fitted a (legend) for each n – shifted up/down by 10^{-2} for clarity. Data for a uniform field XXZ chain with $L = 7$, $L_A = 6$, $J = 1$, $\Delta = 0.95$, and $h_x = h_z = 0.2$.

with the matrix-valued coefficients [52]

$$H_{A,k-1}^* = (-1)^{k-1} \sum_{m=1}^k \frac{(-1)^{m+1}}{m} D_B^m \times \sum_{\{n_1 + \dots + n_m = k\}} \left(\prod_{i=1}^m \frac{\text{tr}_B(H^{n_i})}{n_i!} \right) - [H \leftrightarrow H_B], \quad (8)$$

where the second term, $[H \leftrightarrow H_B]$, is obtained from the first term by replacing H with H_B .

We note that an expansion in a ‘unitful’ quantity β is questionable, and indeed the expansion in Eq. (7) should be in β/J as the dominating scale in the Hamiltonian is J , provided h_j and Δ are not significantly larger than J . In all numerical results, we have chosen $J = 1$, and thus for ease of readability we have opted to omit factors of J .

When the operators in H are trace-less, the first few coefficients are [52]

$$H_{A,0}^* = H_A \quad (9)$$

$$H_{A,1}^* = \frac{1}{2D_B} \text{tr}_B(H_{AB}^2) \quad (10)$$

$$H_{A,2}^* = \frac{1}{6D_B} [\text{tr}_B(H_{AB}H_AH_{AB}) - \text{tr}_B(H_{AB}^2)H_A]. \quad (11)$$

From Eq. (9) one infers the known result $H_A^*(\beta) \rightarrow H_A$ for $\beta \rightarrow 0$ [11, 13], which is illustrated in Fig. 4(a,c).

We denote the overlap of operators O with $H_{A,k}^*$ by $c_k(O) = \text{tr}(OH_{A,k}^*)$, and the smallest $k \geq 1$ such that $c_k(O)$ is non-zero by k_0 . We observed that k_0 is lower bounded by

$$k_0 \geq 2(d+1) - n \quad (12)$$

for n -body operators. In other words, the minimum order at which $c(O)$ can appear is $\mathcal{O}(\beta^{2(d+1)-n})$. Some examples are listed in Table I.

In Fig. 3(a,b) we present $|c(O)|$ as a function of β for $n = 1$ and $n = 2$ operators. For small β , the dependence is a power-law with exponent $2d + 1$ for one-body operators and $2d$ for two-body operators O (dashed-line). Similarly, we find that $c(O)$ is of order $\mathcal{O}(\beta^{2d-1})$ for three-body and $\mathcal{O}(\beta^{2d-2})$ for four-body operators [52]. In addition to these examples obeying the equality in Eq. (12), we also have cases where k_0 is larger than the lower bound: for mixed two-body operators $\sigma_j^\alpha \sigma_{\ell'}^{\alpha'}$ with $\alpha \neq \alpha'$, $c(O)$ follows a power-law in β with exponent $2d + 1$ ($2d + 2$ if $\ell = L_A$) [52].

Before justifying the lower bound, Eq. (12), we first highlight a consequence. We denote $k_0 = 2d + b$, where b is an integer, independent of d and β . Then

$$c(O) = e^{2d \ln \beta} \sum_{k=b}^{\infty} c_{k+2d} \beta^k. \quad (13)$$

We write the d -dependence of the second factor as $|\sum_{k=b}^{\infty} c_{k+2d} \beta^k| \sim e^{-ad}$, where a is a real number; we assume that there is no faster dependence on d . (The prefactor may have polynomial dependence.) Then the exponential dependence of $|c(O)|$ on d is given by

$$|c(O)| \sim e^{-(a-2 \ln \beta)d}. \quad (14)$$

Extracting d_c from Eq. (14) implies Eq. (6). For small β , retaining only the first term in the sum in Eq. (13), we see that a is independent of β for small β [52]. Numerically (Fig. 2(b)), a appears to be β -independent at all β .

B. Justification of the lower bound (12)

Eq. (12) is consistent with the lowest-order expressions, Eqs. (9)-(11). By Eq. (12), two-body Pauli operators with distance $d > 1$ and one-body operators with $d \geq 1$ should have $c_k(O) = 0$ for $k = 1, 2$. These operators are not the identity. But $H_{A,1}^* \propto \mathbb{1}_A$ by Eq. (10), when H_{AB} contains no mixed Pauli operators, so $c_1(O) = 0$. In [52] we show how $c_2(O) = 0$ follows from Eq. (11). For $k > 2$, $H_{A,k}^*$ becomes intractable to calculate. However, we can formulate a heuristic argument for Eq. (12), based on the following

Conjecture. *We express the operator O in terms of tuples h_1, \dots, h_{k+1} up to a constant, $O \equiv h_1 \dots h_{k+1}$ ($k \geq 1$), where the h_i are all in H . If all such tuples h_1, \dots, h_{k+1} can be split into two sets of operators $\mathcal{H}_1 \neq \emptyset$ and \mathcal{H}_2 , such that operators in \mathcal{H}_1 commute with operators in \mathcal{H}_2 and operators in \mathcal{H}_1 have no support in B , then $c_k(O) = 0$.*

The conjecture is supported by the $k = 1$ and $k = 2$ cases, which follow from Eqs. (10) and (11) [52].

As shown visually in Fig. 3(c), the smallest k such that there exists a string $h_1 \dots h_{k+1} \equiv O$, which cannot be separated into $\mathcal{H}_{1,2}$ is given by $k = 2d$ for nearest-neighbor two-body operators $O = \sigma_j^\alpha \sigma_{j+1}^{\alpha'}$ and $k = 2d + 1$

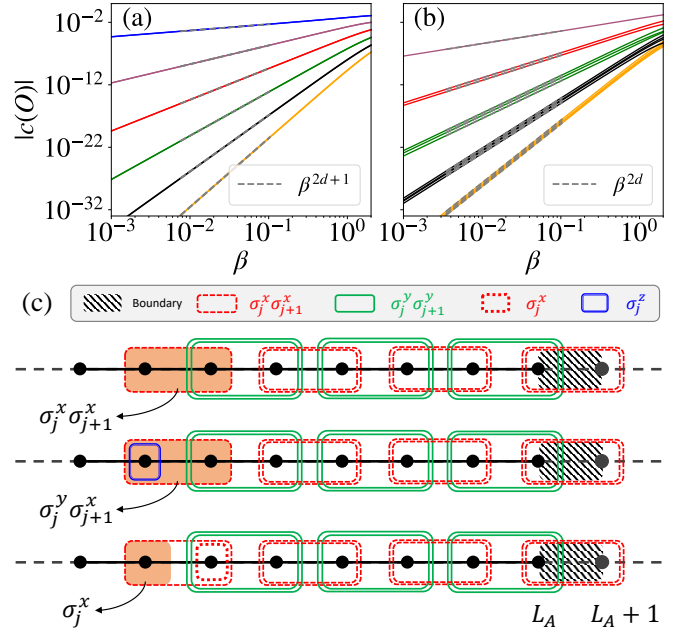


FIG. 3. $|c(O)|$ for (a) 1-body ($\sigma_j^{(x,z)}$) and (b) 2-body ($\sigma_j^\alpha \sigma_{j+1}^{\alpha'}$) operators in H_A^* versus β - Uniform field XXZ chain with $L = 7$, $L_A = 6$, $J = 1$, $\Delta = 0.95$, $h_x = h_z = 0.2$. Similar results are observed in an XXZ chain with disordered fields [52]. Lines are grouped into colors representing the distance to the boundary, the top group being closest to the boundary. (c) Illustration of analytical argument for the factor of $2d$. Rectangles denote Pauli operators (h_i) in H . The different colored patterns correspond to x, y, z , and the enclosed black dots indicate the support of the operator on the chain. Double rectangles mean that the operators appear twice. The orange-shaded regions indicate support of operators corresponding to the product of all Pauli operators in the string ($O \equiv h_1, \dots, h_{k+1}$).

for single-body operators O and mixed nearest-neighbor two-body operators $O = \sigma_j^\alpha \sigma_{j+1}^{\alpha'}$ with $\alpha \neq \alpha'$. These strings are given by nearest neighbor two-body operators appearing in H connecting the bath to the support of the operator O . We sketch such strings in Fig. 3(c) for $O = \sigma_j^x \sigma_{j+1}^x$, $O = \sigma_j^y \sigma_{j+1}^y$ and $O = \sigma_j^x$.

The first row of Fig. 3(c) corresponds to representations of $O = \sigma_j^x \sigma_{j+1}^x$ of the form

$$\sigma_j^x \sigma_{j+1}^x \equiv \sigma_j^x \sigma_{j+1}^x (\sigma_{j+1}^y \sigma_{j+2}^y)^2 \dots (\sigma_{L_A}^{(x/y)} \sigma_{L_A+1}^{(x/y)})^2 \quad (15)$$

or permutations thereof. Using squares of pairs requires the least number of Pauli operators that connect to the bath while yielding the identity operator. The square structure in Eq. (15), reflected in the double rectangles in Fig. 3(c), provides a visual interpretation of the factor 2 in the lower bound (12).

The strings for $O = \sigma_j^y \sigma_j^x$ and $O = \sigma_j^x$, also presented in Fig. 3(c) are similar. They differ only by the first term on the right-hand side in Eq. (15), namely $\sigma_j^y \sigma_{j+1}^x \equiv \sigma_j^z \sigma_j^x \sigma_{j+1}^x$ and $\sigma_j^x \equiv \sigma_{j+1}^x \sigma_j^x \sigma_{j+1}^x$. This agrees with our result that single-body and mixed two-body terms only

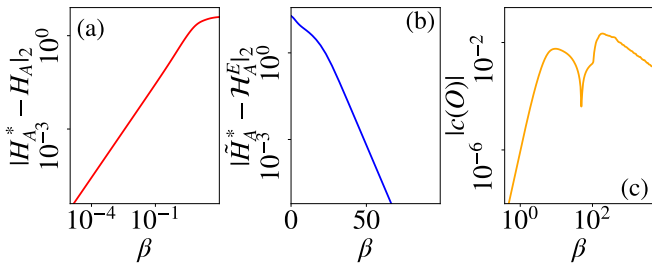


FIG. 4. Hilbert-Schmidt norm of the difference between (a) H_A and H_A^* , (b) \mathcal{H}_A^E and \tilde{H}_A^* , for a uniform field XXZ chain with $L = 7$, $L_A = 3$, $J = 1$, $\Delta = 0.95$, and $h^x = h_z = 0.2$. (c) $|c(O)|$ for a two-body term (that does not appear in H_A) in H_A^* versus β , for the same parameters as (a) and (b) but with $L = 6$ and $L_A = 4$.

appear in the HMF when magnetic fields are present in H [52].

For nearest neighbor two-body operators, $\sigma_j^\alpha \sigma_{j+1}^\alpha$, any Pauli string $h_1 \dots h_{k+1}$ representing the operator with $k < 2d$ can be separated into sets $\mathcal{H}_{1,2}$, because there are not enough operators to construct structures of the type shown in Fig. 3(c). Similarly, for $k < 2d + 1$ this holds for single-body operators and nearest neighbor two-body operators $\sigma_j^\alpha \sigma_{j+1}^{\alpha'}$ with $\alpha \neq \alpha'$.

V. LARGE β

In the limit $\beta \rightarrow \infty$, $e^{-\beta H}/Z$ converges to the projector $P_{GS} = |\Psi_{GS}\rangle\langle\Psi_{GS}|$ onto the ground state subspace, where $|\Psi_{GS}\rangle$ is the ground state wavefunction of the entire $(A + B)$ system. The reduced projector,

$$\rho_A^{GS} = \text{tr}_B(P_{GS}) = \text{tr}_B |\Psi_{GS}\rangle\langle\Psi_{GS}|, \quad (16)$$

i.e., the reduced density matrix of the A region in the ground state wavefunction, is a widely studied object, as it encodes the entanglement between A and B . It is often expressed in terms of an ‘effective’ Hamiltonian \mathcal{H}_A^E , the entanglement Hamiltonian [42–45]:

$$e^{-\mathcal{H}_A^E} = \rho_A^{GS} = \lim_{\beta \rightarrow \infty} \text{tr}_B(e^{-\beta H})Z^{-1}. \quad (17)$$

Comparing with Eq. (1), we obtain the following relationship for $\beta \gg 1$ between the HMF H_A^* and the entanglement Hamiltonian \mathcal{H}_A^E :

$$\mathcal{H}_A^E \approx \beta H_A^* + \ln(Z^*). \quad (18)$$

In other words, the entanglement Hamiltonian is obtained by shifting and scaling the HMF at large β . This relation extends the previously derived result that $H_A^* \propto \mathbb{1}_A$ in the same limit [13].

The shifted and scaled operator $\tilde{H}_A^* = \beta H_A^* + \ln(Z^*)$ is compared in Fig. 4(b) to \mathcal{H}_A^E for $\beta \gg 1$ limit. As predicted, the distance between the two ‘Hamiltonians’ vanishes for $\beta \rightarrow \infty$.

VI. CONCLUDING DISCUSSION

In this work, we investigated the (spatial) structure of the HMF, a fundamental concept in understanding the implications of non-weak coupling in thermodynamics. We demonstrated and explained a skin effect in the HMF structure: The magnitude of terms in $H_A^* - H_A$ decreases exponentially with the distance from the boundary. We also identified the types of terms that can appear in the HMF and at which order they can occur.

The idea of a skin effect in the deviation of the HMF from the system Hamiltonian is related in spirit to ideas discussed in the literature around locality of temperature [53–56]. Since thermal states of systems described by short-range interactions incorporate a notion of locality, it makes sense that the effect on the HMF should be localized near the boundary. To the best of our knowledge, one cannot infer the explicit exponential behavior, Eqs. (5) and (6), from such intuition alone.

While our explicit examples and expressions are for a spin- $\frac{1}{2}$ chain with one-body and nearest-neighbor two-body terms and for traceless operators, it is clear that analogous expressions can be worked out for other cases (fermions, bosons, spins $> \frac{1}{2}$, other local operators, other geometries), and that the physical conclusions are generic.

The form of the skin effect and the skin depth, Eqs. (5) and (6), do not depend on the strength of the ‘system-bath’ coupling H_{AB} . We see from the perturbative construction that the coupling strength can affect the coefficient at most polynomially in d , leaving the exponential decay in Eq. (6) and hence the length d_c unaffected. We have also explicitly tested this independence numerically [52].

Our perturbative construction, and the arguments leading to the skin effect, do not require the subsystem B to be large. Thus, the results are independent of ‘bath size’ in the sense that the form $|c(O)| \sim e^{-d/d_c}$ of Eq. (5), and the value of d_c , are not affected by the size L_B of the B partition [52]. Changing L_B does affect the prefactor in Eq. (5), i.e., the magnitude of $|c(O)|$.

In addition, the chaotic vs. integrable nature of the Hamiltonian, although generally important for thermalization/thermodynamics, plays no role, and our results are independent of integrability.

Our results open up several research directions. (1) The skin effect structure is based on locality; one might ask whether some version of this picture survives for long-ranged Hamiltonians with power-law decay of couplings. (2) Notions of boundary locality have been discussed for the entanglement Hamiltonian and its spectrum [45, 57, 58]. It is intriguing to ask whether these might be related to the skin effect we have presented for the HMF. (3) Numerically, we found the constant a in Eq. (6) to be relatively large (> 1), leading to a rather sharp skin effect (small d_c); the deviations of H_A^* from H_A are strongly localized near the boundary. Whether this is a generic feature for different classes of systems

remains an open question. (4) In this work we have focused on the exponential behavior $|c(O)| \sim e^{-d/d_c}$ and on the constant d_c , and have not attempted to treat the prefactor, i.e., the absolute magnitude of $|c(O)|$, explicitly. For example, the way this prefactor depends on the size of the B partition remains an open question.

ACKNOWLEDGMENTS

PCB acknowledges funding from Science Foundation Ireland through grant 21/RP-2TF/10019. This work was

in part supported by the Deutsche Forschungsgemeinschaft under grant SFB 1143 (project-id 247310070).

-
- [1] F. Binder, L. A. Correa, C. Gogolin, J. Anders, and G. Adesso, eds., *Thermodynamics in the Quantum Regime* (Springer International Publishing, 2018).
- [2] M. Campisi, P. Talkner, and P. Hänggi, Fluctuation theorem for arbitrary open quantum systems, *Phys. Rev. Lett.* **102**, 210401 (2009).
- [3] P. Talkner and P. Hänggi, Colloquium: Statistical mechanics and thermodynamics at strong coupling: Quantum and classical, *Rev. Mod. Phys.* **92**, 041002 (2020).
- [4] J. G. Kirkwood, Statistical mechanics of fluid mixtures, *The Journal of Chemical Physics* **3**, 300 (1935).
- [5] C. Jarzynski, Nonequilibrium work theorem for a system strongly coupled to a thermal environment, *Journal of Statistical Mechanics: Theory and Experiment* **2004**, P09005 (2004).
- [6] M. E. Tuckerman, *Statistical Mechanics: Theory and Molecular Simulation* (Oxford University Press, 2010).
- [7] M. F. Gelin and M. Thoss, Thermodynamics of a subensemble of a canonical ensemble, *Phys. Rev. E* **79**, 051121 (2009).
- [8] S. Hilt, B. Thomas, and E. Lutz, Hamiltonian of mean force for damped quantum systems, *Phys. Rev. E* **84**, 031110 (2011).
- [9] R. Gallego, A. Riera, and J. Eisert, Thermal machines beyond the weak coupling regime, *New Journal of Physics* **16**, 125009 (2014).
- [10] A. Rivas, Strong coupling thermodynamics of open quantum systems, *Phys. Rev. Lett.* **124**, 160601 (2020).
- [11] J. D. Cresser and J. Anders, Weak and ultrastrong coupling limits of the quantum mean force Gibbs state, *Phys. Rev. Lett.* **127**, 250601 (2021).
- [12] Y.-F. Chiu, A. Strathearn, and J. Keeling, Numerical evaluation and robustness of the quantum mean-force Gibbs state, *Phys. Rev. A* **106**, 012204 (2022).
- [13] T. Chen and Y.-C. Cheng, Numerical computation of the equilibrium-reduced density matrix for strongly coupled open quantum systems, *The Journal of Chemical Physics* **157**, 064106 (2022).
- [14] A. E. Teretenkov, Effective gibbs state for averaged observables, *Entropy* **24**, 10.3390/e24081144 (2022).
- [15] A. S. Trushechkin, M. Merkli, J. D. Cresser, and J. Anders, Open quantum system dynamics and the mean force gibbs state, *AVS Quantum Science* **4**, 012301 (2022).
- [16] G. M. Timofeev and A. S. Trushechkin, Hamiltonian of mean force in the weak-coupling and high-temperature approximations and refined quantum master equations, *International Journal of Modern Physics A* **37**, 2243021 (2022).
- [17] J. S. Lee and J. Yeo, Perturbative steady states of completely positive quantum master equations, *Phys. Rev. E* **106**, 054145 (2022).
- [18] N. Anto-Sztrikacs, A. Nazir, and D. Segal, Effective-hamiltonian theory of open quantum systems at strong coupling, *PRX Quantum* **4**, 020307 (2023).
- [19] L. D'Alessio, Y. Kafri, A. Polkovnikov, and M. Rigol, From quantum chaos and eigenstate thermalization to statistical mechanics and thermodynamics, *Advances in Physics* **65**, 239 (2016).
- [20] R. Nandkishore and D. A. Huse, Many-body localization and thermalization in quantum statistical mechanics, *Annual Review of Condensed Matter Physics* **6**, 15 (2015).
- [21] M. P. Müller, E. Adlam, L. Masanes, and N. Wiebe, Thermalization and canonical typicality in translation-invariant quantum lattice systems, *Communications in Mathematical Physics* **340**, 499 (2015).
- [22] A. M. Kaufman, M. E. Tai, A. Lukin, M. Rispoli, R. Schittko, P. M. Preiss, and M. Greiner, Quantum thermalization through entanglement in an isolated many-body system, *Science* **353**, 794 (2016).
- [23] A. Dymarsky, N. Lashkari, and H. Liu, Subsystem eigenstate thermalization hypothesis, *Phys. Rev. E* **97**, 012140 (2018).
- [24] J. R. Garrison and T. Grover, Does a single eigenstate encode the full Hamiltonian?, *Phys. Rev. X* **8**, 021026 (2018).
- [25] P. C. Burke, G. Nakerst, and M. Haque, Assigning temperatures to eigenstates, *Phys. Rev. E* **107**, 024102 (2023).
- [26] M. Rigol, V. Dunjko, and M. Olshanii, Thermalization and its mechanism for generic isolated quantum systems, *Nature* **452**, 854 (2008).
- [27] M. Rigol, Breakdown of thermalization in finite one-dimensional systems, *Phys. Rev. Lett.* **103**, 100403 (2009).
- [28] M. Rigol, Quantum quenches and thermalization in one-dimensional fermionic systems, *Phys. Rev. A* **80**, 053607 (2009).
- [29] M. Rigol and L. F. Santos, Quantum chaos and thermalization in gapped systems, *Phys. Rev. A* **82**, 011604 (2010).
- [30] L. F. Santos and M. Rigol, Onset of quantum chaos in one-dimensional bosonic and fermionic systems and

- its relation to thermalization, *Phys. Rev. E* **81**, 036206 (2010).
- [31] G. Roux, Finite-size effects in global quantum quenches: Examples from free bosons in an harmonic trap and the one-dimensional Bose-Hubbard model, *Phys. Rev. A* **81**, 053604 (2010).
- [32] M. Rigol and M. Srednicki, Alternatives to eigenstate thermalization, *Phys. Rev. Lett.* **108**, 110601 (2012).
- [33] L. F. Santos, A. Polkovnikov, and M. Rigol, Weak and strong typicality in quantum systems, *Phys. Rev. E* **86**, 010102 (2012).
- [34] C. Neuenhahn and F. Marquardt, Thermalization of interacting fermions and delocalization in Fock space, *Phys. Rev. E* **85**, 060101 (2012).
- [35] E. Khatami, G. Pupillo, M. Srednicki, and M. Rigol, Fluctuation-dissipation theorem in an isolated system of quantum dipolar bosons after a quench, *Phys. Rev. Lett.* **111**, 050403 (2013).
- [36] S. Sorg, L. Vidmar, L. Pollet, and F. Heidrich-Meisner, Relaxation and thermalization in the one-dimensional Bose-Hubbard model: A case study for the interaction quantum quench from the atomic limit, *Phys. Rev. A* **90**, 033606 (2014).
- [37] K. R. Fratus and M. Srednicki, Eigenstate thermalization in systems with spontaneously broken symmetry, *Phys. Rev. E* **92**, 040103 (2015).
- [38] F. H. L. Essler and M. Fagotti, Quench dynamics and relaxation in isolated integrable quantum spin chains, *Journal of Statistical Mechanics: Theory and Experiment* **2016**, 064002 (2016).
- [39] T.-C. Lu and T. Grover, Renyi entropy of chaotic eigenstates, *Phys. Rev. E* **99**, 032111 (2019).
- [40] K. Seki and S. Yunoki, Emergence of a thermal equilibrium in a subsystem of a pure ground state by quantum entanglement, *Phys. Rev. Research* **2**, 043087 (2020).
- [41] J. D. Noh, Eigenstate thermalization hypothesis and eigenstate-to-eigenstate fluctuations, *Phys. Rev. E* **103**, 012129 (2021).
- [42] H. Li and F. D. M. Haldane, Entanglement spectrum as a generalization of entanglement entropy: Identification of topological order in non-abelian fractional quantum hall effect states, *Phys. Rev. Lett.* **101**, 010504 (2008).
- [43] I. Peschel and V. Eisler, Reduced density matrices and entanglement entropy in free lattice models, *Journal of Physics A: Mathematical and Theoretical* **42**, 504003 (2009).
- [44] V. Eisler and I. Peschel, Properties of the entanglement hamiltonian for finite free-fermion chains, *Journal of Statistical Mechanics: Theory and Experiment* **2018**, 104001 (2018).
- [45] M. Dalmonte, V. Eisler, M. Falconi, and B. Vermersch, Entanglement hamiltonians: From field theory to lattice models and experiments, *Annalen der Physik* **534**, 2200064 (2022).
- [46] P. Strasberg and M. Esposito, Measurability of nonequilibrium thermodynamics in terms of the hamiltonian of mean force, *Phys. Rev. E* **101**, 050101 (2020).
- [47] P. Talkner and P. Hänggi, Comment on “measurability of nonequilibrium thermodynamics in terms of the hamiltonian of mean force”, *Phys. Rev. E* **102**, 066101 (2020).
- [48] P. Strasberg and M. Esposito, Reply to “comment on ‘measurability of nonequilibrium thermodynamics in terms of the hamiltonian of mean force’ ”, *Phys. Rev. E* **102**, 066102 (2020).
- [49] S. Goldstein, J. L. Lebowitz, R. Tumulka, and N. Zanghì, Canonical typicality, *Phys. Rev. Lett.* **96**, 050403 (2006).
- [50] S. Popescu, A. J. Short, and A. Winter, Entanglement and the foundations of statistical mechanics, *Nature Physics* **2**, 754 (2006).
- [51] T. Mori, T. N. Ikeda, E. Kaminishi, and M. Ueda, Thermalization and prethermalization in isolated quantum systems: a theoretical overview, *Journal of Physics B: Atomic, Molecular and Optical Physics* **51**, 112001 (2018).
- [52] See Supplemental Materials for further information.
- [53] M. Kliesch, C. Gogolin, M. J. Kastoryano, A. Riera, and J. Eisert, Locality of temperature, *Phys. Rev. X* **4**, 031019 (2014).
- [54] S. Hernández-Santana, A. Riera, K. V. Hovhannisyan, M. Perarnau-Llobet, L. Tagliacozzo, and A. Acín, Locality of temperature in spin chains, *New Journal of Physics* **17**, 085007 (2015).
- [55] G. De Palma, A. De Pasquale, and V. Giovannetti, Universal locality of quantum thermal susceptibility, *Phys. Rev. A* **95**, 052115 (2017).
- [56] A. M. Alhambra, Quantum many-body systems in thermal equilibrium, *PRX Quantum* **4**, 040201 (2023).
- [57] V. Alba, M. Haque, and A. M. Läuchli, Boundary-locality and perturbative structure of entanglement spectra in gapped systems, *Phys. Rev. Lett.* **108**, 227201 (2012).
- [58] V. Alba, M. Haque, and A. M. Läuchli, Entanglement spectrum of the two-dimensional bose-hubbard model, *Phys. Rev. Lett.* **110**, 260403 (2013).

Supplemental Material for *Structure of the Hamiltonian of mean force*

S.I. OVERVIEW

In the Supplemental Material, we provide supporting information and data.

- In Section [S.II](#) we explain which terms can and cannot appear in the Hamiltonian of mean force for the *XXZ* chain.
- In Section [S.III](#) we provide the small β expansion of the HMF. We further prove the “lower bound” and the conjecture in the main text for $k = 1$ and $k = 2$.
- In Section [S.IV](#) we provide additional data for different n -body coefficients in the HMF.
- In Section [S.V](#) we present some data for a disordered field model.
- In Section [S.VI](#) we show the result of tuning the coupling J_{AB} .

S.II. ZERO COEFFICIENTS OF *XXZ* MODEL WITHOUT MAGNETIC FIELDS

In this section, we show that single-body and two-body mixed Pauli operators do not appear in the HMF of the

XXZ model without magnetic fields. The result is independent of the geometry of the underlying lattice.

Let us first define a ‘sign’ of a Pauli operator σ^α , where $\alpha \in \{0, x, y, z\}$,

$$s(\sigma^\alpha) = \begin{cases} 1 & \alpha = 0 \text{ or } x \\ -1 & \alpha = y \text{ or } z. \end{cases} \quad (\text{S.1})$$

The choice of which operator to assign $+1$ is arbitrary. The identity has to have $s = +1$. The two other Pauli operators will be assigned $s = -1$. In the following we will interpret the spin algebra $\mathfrak{su}(2)$ with the Klein four-group by identifying $\sigma^x \sigma^y \equiv \sigma^y \sigma^x \equiv \sigma^z$ and equivalently for the other Pauli operators. Then it is easy to see that s is a homomorphism on the Klein group, i.e. for $\alpha, \alpha' \in \{0, x, z, y\}$,

$$s(\sigma^\alpha \sigma^{\alpha'}) = s(\sigma^\alpha) s(\sigma^{\alpha'}). \quad (\text{S.2})$$

This homomorphism is generalized to Pauli strings via

$$s\left(\prod_i \sigma_i^{\alpha_i}\right) = \prod_i s(\sigma_i^{\alpha_i}). \quad (\text{S.3})$$

Obviously, all Pauli operators in the XXZ Hamiltonian H_{XXZ} without magnetic fields have $s = +1$. By the homomorphism property of s , this generalizes to all Pauli operators in powers of H_{XXZ} . Together with the fact that \exp is an analytic function, this implies that $\exp(-\beta H_{XXZ})$ only contains Pauli operators with $s = +1$.

The partial trace tr_B is a projection, such that for every Pauli operator σ , $\text{tr}_B(\sigma) = \sigma$, if and only if σ has no support on B , and $\text{tr}_B(\sigma) = 0$ otherwise. Especially, tr_B preserves s , whenever the Pauli operator σ is not projected onto 0. Thus, $\text{tr}_B(\exp(-\beta H_{XXZ}))$ only contains Pauli operators with $s = +1$.

Again, by exploiting the homomorphism property of s and that \log is an analytic function, all Pauli operators in the HMF of the XXZ model without magnetic fields have $s = +1$. This excludes especially $\sigma^{y,z}$ and $\sigma_i^x \sigma_j^y$, $\sigma_i^x \sigma_j^z$ for $i \neq j$.

The above arguments are invariant under interchanging x, y, z arbitrarily while keeping the assignment of signs such that one Pauli operator has $s = +1$ and the two other non-trivial ones have $s = -1$. Thus the HMF of the XXZ model without magnetic fields does not contain any single-body terms nor mixed two-body terms $\sigma_i^\alpha \sigma_j^{\alpha'}$ with $\alpha \neq \alpha'$. Further, 3-body and 4-body terms with positive signs for any sign function like $\sigma^x \sigma^y \sigma^z$ and $\sigma^x \sigma^y \sigma^x \sigma^y$ do appear, while terms like $\sigma^x \sigma^x \sigma^y$ or $\sigma^x \sigma^y \sigma^x \sigma^z$, which can have negative signs, do not.

S.III. SMALL β EXPANSION OF THE HMF

In this section, we derive the expansion of the HMF around $\beta = 0$ and the explicit forms of the matrix-valued coefficients $H_{A,k}^*$ for $k = 0, 1, 2$, utilized in the main text.

Recall the definition of the HMF, presented in the main text,

$$H_A^*(\beta) = -\frac{1}{\beta} \ln \frac{\text{tr}_B(e^{-\beta H})}{\text{tr}_B(e^{-\beta H_B})}. \quad (\text{S.4})$$

We can separate the logarithm into two terms, as the denominator is simply a number, giving

$$H_A^* = -\beta^{-1} (\ln(\text{tr}_B e^{-\beta H}) - \ln(\text{tr}_B e^{-\beta H_B}) \cdot \mathbb{1}_A). \quad (\text{S.5})$$

Now, to evaluate this, we shall write down the full power series of the matrix exponential

$$\begin{aligned} \text{tr}_B e^{-\beta H} &= \text{tr}_B \sum_{n=0}^{\infty} \frac{(-\beta H)^n}{n!} \\ &= D_B \mathbb{1}_A + \sum_{n=1}^{\infty} \text{tr}_B \frac{(-\beta H)^n}{n!} \end{aligned} \quad (\text{S.6})$$

and logarithm

$$\ln(\mathbb{1} + X) = \sum_{n=1}^{\infty} \frac{(X)^n (-1)^{n+1}}{n}. \quad (\text{S.7})$$

Following some algebra, one obtains for the first term in Eq. (S.5)

$$\begin{aligned} \ln(\text{tr}_B e^{-\beta H}) &= \sum_{k=1}^{\infty} (-\beta)^k \sum_{m=1}^k D_B^{-m} \frac{(-1)^{m+1}}{m} \\ &\quad \sum_{\{n_1+\dots+n_m=k\}} \left(\prod_{i=1}^m \frac{\text{tr}_B(H^{n_i})}{n_i!} \right), \end{aligned} \quad (\text{S.8})$$

where the last sum is over all integers $n_1, \dots, n_m \geq 1$ with $n_1 + \dots + n_m = k$. The second term is retrieved similarly by replacing H with H_B . Thus, the Hamiltonian of mean force is

$$\begin{aligned} H_A^* &= \sum_{k=1}^{\infty} (-\beta)^{k-1} \sum_{m=1}^k D_B^{-m} \frac{(-1)^{m+1}}{m} \\ &\quad \sum_{\{n_1+\dots+n_m=k\}} \left(\prod_{i=1}^m \frac{\text{tr}_B(H^{n_i})}{n_i!} \right) \\ &\quad - \sum_{k=1}^{\infty} (-\beta)^{k-1} \sum_{m=1}^k D_B^{-m} \frac{(-1)^{m+1}}{m} \\ &\quad \sum_{\{n_1+\dots+n_m=k\}} \left(\prod_{i=1}^m \frac{\text{tr}_B(H_B^{n_i})}{n_i!} \right) \\ &= \sum_{k=0}^{\infty} \beta^k H_{A,k}^*, \end{aligned} \quad (\text{S.9})$$

with

$$\begin{aligned} H_{A,k-1}^* &= (-1)^{k-1} \sum_{m=1}^k \frac{(-1)^{m+1}}{m} D_B^m \\ &\quad \sum_{\{n_1+\dots+n_m=k\}} \left[\prod_{i=1}^m \frac{\text{tr}_B(H^{n_i})}{n_i!} - \prod_{i=1}^m \frac{\text{tr}_B(H_B^{n_i})}{n_i!} \right] \end{aligned} \quad (\text{S.10})$$

Proceeding, we assume that the terms in the Hamiltonian H are traceless. This is of course true for spin-1/2 systems.

The zeroth order term is then calculated as

$$H_{A,0}^* = \frac{1}{D_B} (\text{tr}_B(H) - \text{tr}_B(H_B)) = H_A, \quad (\text{S.11})$$

where we used $\text{tr}_B(H_{AB}) = 0$. The first-order term is given by

$$\begin{aligned} H_{A,1}^* &= - \left(\frac{\text{tr}_B(H^2)}{2D_B} - \frac{\text{tr}_B(H_B^2)}{2D_B} - \frac{(\text{tr}_B H)^2}{2D_B^2} \right) \\ &= \frac{1}{2} \left(H_A^2 + \frac{\text{tr}_B(H_B^2)}{D_B} - \frac{D_B H_A^2 + \text{tr}_B(H_B^2 + H_{AB}^2)}{D_B} \right) \\ &= \frac{1}{2D_B} \text{tr}_B(H_{AB}^2). \end{aligned} \quad (\text{S.12})$$

If the boundary term H_{AB} does only contain non-mixed terms $\sigma_i^\alpha \sigma_j^\alpha$ for $\alpha \in \{x, y, z\}$ then $\text{tr}_B(H_{AB}^2) \propto \mathbb{1}_A$, so we get

$$H_{A,1}^* \propto \mathbb{1}_A. \quad (\text{S.13})$$

The second-order term is given by

$$\begin{aligned} H_{A,2}^* &= - \left[\left(\frac{\text{tr}_B H^3}{3!D_B} \right) + \left(\frac{(\text{tr}_B H)^3}{3D_B^3} \right) - \right. \\ &\quad \left. \frac{1}{2D_B^2} (\text{tr}_B H \cdot \text{tr}_B H^2/2 + \text{tr}_B H^2 \cdot \text{tr}_B H/2) \right] \\ &= \left[\frac{H_A^3}{3} + \frac{\text{tr}_B H^3}{6D_B} - \frac{1}{4D_B} [H_A, \text{tr}_B H^2]_+ \right] \\ &= \left[\frac{4H_A^3}{12} + \frac{2\text{tr}_B H^3}{12D_B} - \frac{3}{12D_B} [H_A, \text{tr}_B H^2]_+ \right], \end{aligned} \quad (\text{S.14})$$

where $[A, B]_+ = AB + BA$ is an anticommutator. The first two terms will contain $\frac{6}{12} H_A^3$ and the anticommutator will contain $\frac{3}{12} \cdot 2H_A^3$, so all powers of H_A cancel. Evaluating the term we get up to a constant shift

$$H_{A,2}^* = \frac{1}{6D_B} (\text{tr}_B(H_{AB}H_AH_{AB}) - \text{tr}_B(H_{AB}^2) \cdot H_A). \quad (\text{S.15})$$

S.III.A. Lowest-order expressions and the ‘‘lower bound’’

In the following, we show that the lower bound on k such that $c_k(O) = \text{tr}(OH_{A,k}^*) \neq 0$ is consistent with the explicit forms of $H_{A,k}^*$ for $k = 1, 2$. Namely, we show for Pauli operators with $d(O) > 1$ ($d(O) \geq 1$ for single-body Pauli operators) that $c_k(O) = 0$ for $k = 1, 2$.

First, the statement is trivial for $k = 1$ as $H_{A,1}^*$ is proportional to the identity operator, whenever H_{AB} does not contain mixed Pauli operators.

So let us turn to $H_{A,2}^*$. We expand H_A in terms of operators h_A , which are proportional to Pauli operators, $H_A = \sum_{h_A} h_A$. By separating the sum over h_A 's into h_A 's commuting and not commuting with H_{AB} one easily sees that only the non-commuting h_A 's are contributing to $H_{A,2}^*$,

$$\sum_{h_A: [h_A, H_{AB}] = 0} [\text{tr}_B(H_{AB}h_AH_{AB}) - \text{tr}_B(H_{AB}^2) \cdot h_A] = 0, \quad (\text{S.16})$$

so $c_2(O)$ is proportional to

$$\sum_{h_A: [h_A, H_{AB}] \neq 0} \text{tr}(O[\text{tr}_B(H_{AB}h_AH_{AB}) - \text{tr}_B(H_{AB}^2) \cdot h_A]). \quad (\text{S.17})$$

Recall that $\text{tr}(O_1O_2) \neq 0$ for two Pauli operators O_1, O_2 implies that O_1 equals O_2 up to a multiplicative factor. Especially, the supports of both operators have to coincide.

Let us now restrict to Hamiltonians H with only nearest neighbor terms. Then all h_A not commuting with H_{AB} have support contained in $[L_A - 1, L_A]$. The same holds for the supports of $\text{tr}_B(H_{AB}h_AH_{AB})$ and $\text{tr}_B(H_{AB}^2) \cdot h_A$. But for a Pauli operator O with $d(O) > 1$, the support of O is by definition of the distance d not contained in $[L_A - 1, L_A]$. Thus the support of O does not coincide with the support of $\text{tr}_B(H_{AB}h_AH_{AB})$ nor with the support of $\text{tr}_B(H_{AB}^2) \cdot h_A$. By the argument in the previous paragraph, $\text{tr}(O \text{tr}_B(H_{AB}h_AH_{AB})) = \text{tr}(O \text{tr}_B(H_{AB}^2) \cdot h_A) = 0$, so $c_2(O) = 0$.

Finally, consider a single-body Pauli operator O with $d(O) = 1$. Then O is supported only on-site $L_A - 1$ and commutes with H_{AB} . If the boundary term H_{AB} contains only non-mixed terms $\sigma_i^\alpha \sigma_j^\alpha$ for $\alpha \in \{x, y, z\}$ then $\text{tr}_B(H_{AB}h_AH_{AB}) \propto \text{tr}_B(H_{AB}^2)h_A \propto h_A$. But the sum in Eq. (S.17) only runs over h_A , which are *not* commuting with H_{AB} . Thus O and h_A are not proportional and so $c_2(O) = 0$.

S.III.B. Conjecture for $k = 1, 2$

In this subsection, our objective is to demonstrate that the conjecture presented in the main text holds for cases where $k = 1$ and $k = 2$. We restrict to operators O which are supported in A as otherwise $c_k(O) = 0$ holds trivially for all k .

Let us first consider $k = 1$ and an operator O that meets the conjecture's prerequisites. It follows that O cannot be the identity operator, as the identity can always be expressed as $\text{Id} = h_{AB}^2$, where h_{AB} is any Pauli operator in H with support in A and B . In the absence of any mixed terms within H_{AB} , it follows that $H_{A,1}^* \propto \text{tr}_B(H_{AB}^2) \propto \text{Id}$, leading to the conclusion that $c_1(O) = \text{tr}(OH_{A,1}^*) = 0$.

Now, let us consider $k = 2$. Our goal is to demonstrate that an operator O fulfilling the conjecture's conditions implies $d(O) > 1$ ($d(O) \geq 1$ for single-body operators O).

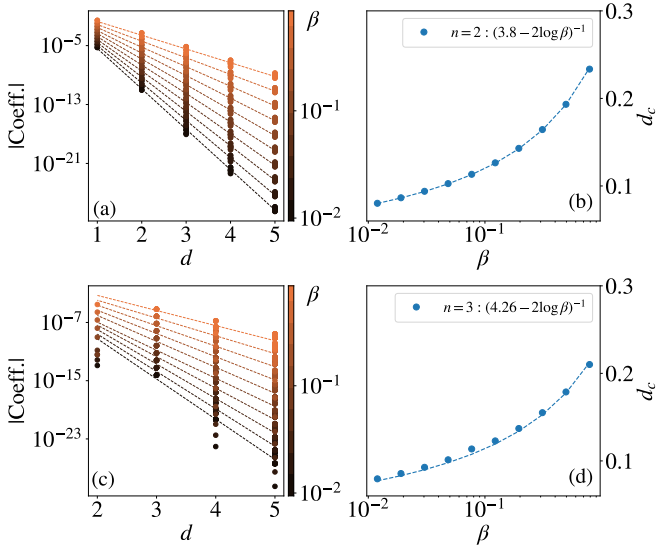


FIG. S1. Magnitude of (a) 2-body ($\sigma_j^\alpha \sigma_k^\alpha$) and (c) 3-body ($\sigma_j^\alpha \sigma_k^\alpha \sigma_\ell^{\alpha'}$) coefficients in the Hamiltonian of mean force plotted versus distance over a range of β . (b,d) The slope of the lines of best fit to the data in (a,c) is plotted as a function of β . – Uniform field XXZ chain with $L = 7$, $L_A = 6$, $J = 1$, $\Delta = 0.95$, $h_x = h_z = 0.2$.

In that case, the preceding subsection’s arguments imply that $c_2(O) = 0$. We will verify the previous statement through contra-position: if O is a single-body operator and $d(O) = 0$, then O is supported on L_A . Conversely, if O is not a single-body operator and $d(O) = 1$ then O is a two-body operator and has support on L_A . Take any term h_{AB} in H , which is supported on the boundary of A and B and does not commute with the single-body Pauli operator of O on L_A . Then $O \equiv Oh_{AB}^2$ cannot be decomposed into the set \mathcal{H}_1 and \mathcal{H}_2 as outlined in the conjecture. This completes the proof.

S.IV. ADDITIONAL DATA FOR N-BODY TERMS

Here, we provide further data for different n -body terms for the ‘uniform field’ XXZ chain, complementing what is already presented in the main text.

Firstly, in Fig. S1(a,c), we plot the coefficients of two and three-body terms as a function of the distance d to the boundary. In (b,d), we plot the value of d_c as a function of β , again illustrating the form $d_c = (a - 2 \log \beta)^{-1}$ presented in the main text.

Then, in Fig. S2, we plot the coefficients of three-body (a) and four-body (b) terms as a function of β , highlighting again the $\beta^{2(d+1)-n}$ behavior.

Finally, in Fig. S3, we plot the coefficients of the mixed 2-body terms as a function of β , illustrating that they do not follow equality with the lower bound of β^{2d} . Fig. S3(a) shows that non-boundary terms scale as β^{2d+1} ,

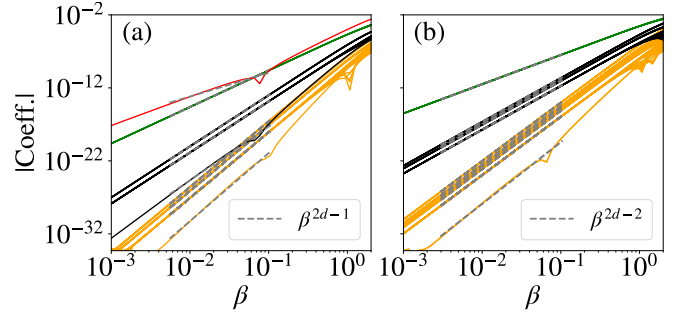


FIG. S2. Magnitude of (a) 3-body ($\sigma_j^\alpha \sigma_k^\alpha \sigma_\ell^{\alpha'}$) and (b) 4-body ($\sigma_j^\alpha \sigma_k^\alpha \sigma_\ell^{\alpha'} \sigma_m^{\alpha'}$) coefficients in the Hamiltonian of mean force plotted versus β - Uniform field XXZ chain with $L = 7$, $L_A = 6$, $J = 1$, $\Delta = 0.95$, $h_x = h_z = 0.2$. In each panel, each group of lines is colored with respect to the distance from the boundary, with the top group of lines being the closest to the boundary.

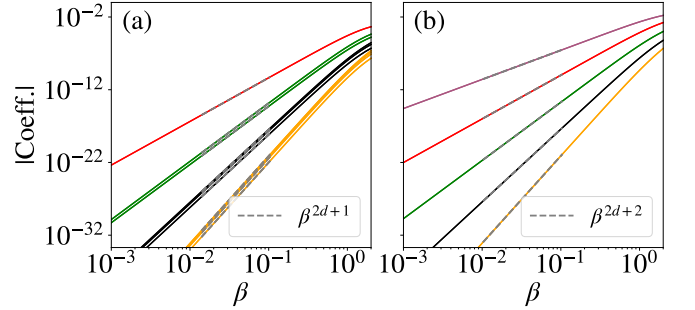


FIG. S3. Magnitude of 2-body coefficients, (a) $\sigma_j^\alpha \sigma_k^{\alpha'}$ and (b) $\sigma_j^\alpha \sigma_{L_A}^{\alpha'}$, in the Hamiltonian of mean force plotted versus β - Uniform field XXZ chain with $L = 7$, $L_A = 6$, $J = 1$, $\Delta = 1$, $h^x = h^z = 1$. In each panel, each group of lines is colored with respect to the distance from the boundary, with the top group of lines being the closest to the boundary.

while (b) shows that boundary terms scale as β^{2d+2} .

S.V. ADDITIONAL DATA FOR DISORDERED FIELD MODEL

In the main text, we introduced the XXZ chain with the addition of transverse and longitudinal magnetic fields,

$$H = J \sum_{j=1}^{L-1} (\sigma_j^x \sigma_{j+1}^x + \sigma_j^y \sigma_{j+1}^y) + \Delta \sum_{j=1}^{L-1} \sigma_j^z \sigma_{j+1}^z + \sum_{j=1}^L (h_j^z \sigma_j^z + h_j^x \sigma_j^x). \quad (\text{S.18})$$

We generally presented data for the case of uniform magnetic field strength across the lattice, however, we have checked our results for various parameters. In Figures S4-S5, we present results using Eq. (S.18) with *disor-*

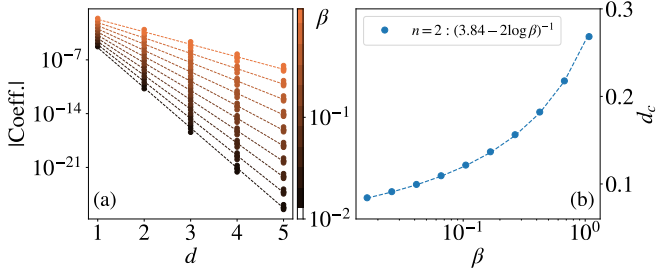


FIG. S4. (a) Magnitude of two-body coefficients ($\sigma_j^x \sigma_k^x$) in the HMF versus distance for different β (colorbar). (b) Skin depth d_c (dots) as a function of β . $n = 1$ corresponds to slopes in (a). Dashed lines are $(a - 2 \log \beta)^{-1}$ for fitted a (legend). Data for a disordered field XXZ chain with $L = 7$, $L_A = 6$, $J = 1$, $\Delta = 0.95$, and $h_x = h_z = 0.2$.

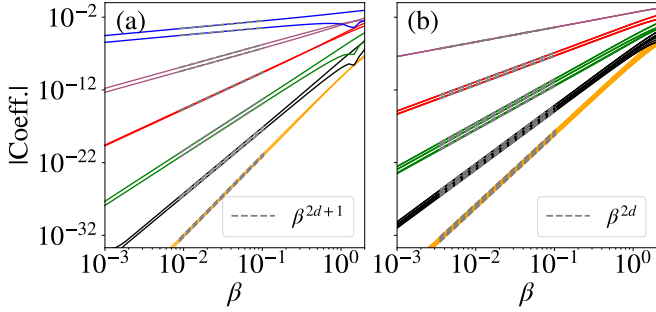


FIG. S5. Magnitude of (a) 1-body (σ_j^x) and (b) 2-body ($\sigma_j^x \sigma_k^x$) coefficients in the Hamiltonian of mean force plotted versus β - Disordered field XXZ chain with $L = 7$, $L_A = 6$, $J = 1$, $\Delta = 0.95$, $h_j^x, h_j^z \in [-0.2, 0.2]$. In each panel, each group of lines is colored with respect to the distance from the boundary, with the top group of lines being the closest to the boundary.

dered magnetic fields, $h_j^z \in [-h^z, h^z]$, $h_j^x \in [-h^x, h^x]$. In Fig. S4 (a), we plot the coefficients of one-body terms versus the distance d to the boundary for various β values. In (b), we plot d_c as a function of β , illustrating the $a - 2 \log \beta$ behavior. In Fig. S5, we plot the coefficients of one and two-body terms as a function of β .

S.VI. TUNING COUPLING STRENGTH

In the main text, we stated that the strength of the interaction, J_{AB} , does not affect our presented results. In particular, while the magnitude of the coefficients will change, the value of d_c does not change with J_{AB} . In Fig. S6 (a), we show the value of two-body coefficients as a function of distance d for various J_{AB} at $\beta = 0.1672$. One can see from the figure that the lines shift downwards but do not perceptibly change in slope. In (b), the value of d_c is plotted versus J_{AB} , again showing the value hardly changes with decreasing J_{AB} .

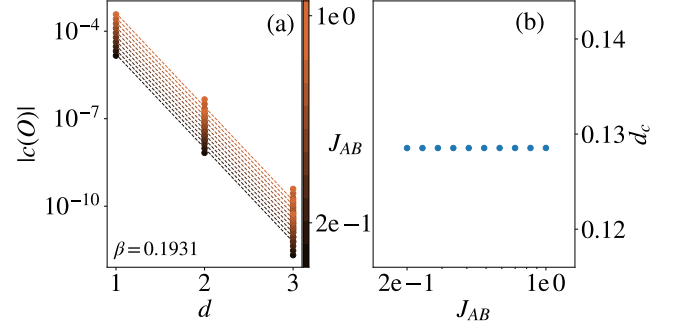


FIG. S6. (a) $|c(O)|$ for 2-body terms ($\sigma_j^x \sigma_k^x$) in the HMF versus distance d for various J_{AB} (colorbar), at fixed $\beta = 0.1931$. (b) Skin depth d_c as a function J_{AB} for the same 2-body terms and temperature as in (a). Data for a uniform field XXZ Chain with $J = 1$, $\Delta = 0.95$, $h_x = h_z = 0.2$, $L = 6$, $L_A = 4$.

S.VII. TUNING BATH SIZE

In the main text, we stated that the size of the bath, L_B , does not affect the exponential behavior detailed therein. In particular, while the magnitude of the coefficients may change, the value of d_c does not meaningfully change with L_B . In Fig. S7 (a), we show the value of two-body coefficients as a function of distance d for various L_B at $\beta = 0.0625$. One can see from the figure that the lines shift downwards but do not perceptibly change in slope. In (b), the value of d_c extracted from the lines in (a) are plotted versus $L_B = L - L_A$. We observe that d_c is essentially constant with increasing L_B . The minor fluctuations can be attributed to errors in the fitting of the lines in (a), however extracting explicit error bars from the data is cumbersome.

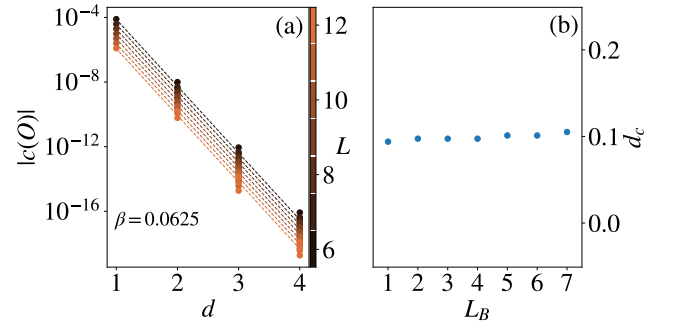


FIG. S7. (a) $|c(O)|$ for 2-body terms ($\sigma_j^x \sigma_k^x$) in the HMF versus distance d for various L (colorbar), at fixed $\beta = 0.0625$. (b) Skin depth d_c as a function $L_B(L)$ for the same 2-body terms and temperature as in (a). Data for a uniform field XXZ Chain with $J = 1$, $\Delta = 0.95$, $h_x = h_z = 0.2$, $L_A = 5$.